11D.3

TROPICAL PRECIPITATION VARIABILITY AND CONVECTIVELY COUPLED EQUATORIAL WAVES IN REANALYSES AND TRMM OBSERVATIONS

Ji-Eun Kim[1] and M. Joan Alexander[2]
[1]Department of Atmospheric and Oceanic Sciences, University of Colorado, Boulder, Colorado
[2]NorthWest Research Associates, Boulder, Colorado

1. INTRODUCTION

Tropical convective systems are often organized by atmospheric waves. In turn, convection generates a broad spectrum of waves that propagate horizontally and vertically. The coupling of convection with waves results in unique frequency characteristics in tropical precipitation. Also, vertically propagating waves, which are preferentially generated by more transient and smaller-scale convective events, have significant impacts on the tropical middle atmosphere and global climate by wave-mean interactions. Despite the importance of generating accurate precipitation in models for weather forecasts and climate projections, there are considerable disagreements between models (Lin 2006; Straub 2010). Moreover, studies about precipitation and convectively coupled equatorial waves (CCEWs) have only focused on intraseasonal or longer time scales (Cho 2004), so there is a lack of observational and model studies for high-frequency precipitation variability as a source and the resulting equatorial waves.

In this study, submonthly scale tropical precipitation variability and CCEW characteristics are investigated using a satellite-derived rainfall estimate, and the result is compared with five reanalyses. Since precipitation in reanalyses is almost entirely a model product, we can evaluate model performance in dealing with convective processes.

2. Datasets and Methodology

We analyzed precipitation data between 15S-15N for the period of January 2005 through December 2007 from five reanalyses: ERA-interim (ERA) (Dee et al. 2011), Modern-Era Retrospective Analysis (MERRA) (Rienecker et al. 2011), National Centers for Environmental Prediction (NCEP)-National Center for Atmospheric and Research (NCEP1) (Kalnay et al. 1996), NCEP-Department of Energy (NCEP2) (Kanamitsu et al. 2002), and NCEP-Climate Forecast System Reanalysis (CFSR) (Saha et al. 2010). We used 6-hourly or 3-hourly products, if available. The reanalysis results were compared with the results of the 3-hourly 3B42 dataset from the Tropical Rainfall Measuring Mission (TRMM) (Huffman et al. 2007).

We performed a spectral analysis for longitude-time cross sections to identify zonally propagating precipitation disturbances. As we are interested not only in CCEW signals but also in precipitation variability and frequency characteristics, we used the raw spectrum without smoothing. Since the prominent lobes in the raw spectrum give information on wave properties, we can also determine whether and how CCEWs are resolved in reanalyses using the raw spectrum. For more reliable quantitative comparisons of variance, we rebinned data in the horizontal to approximately the same resolution of about 1.875°x1.875° for all datasets. Since we are interested in submonthly scale variability and its seasonal changes, the time period of 36 days was chosen for the spectral analysis with 6-day overlap.

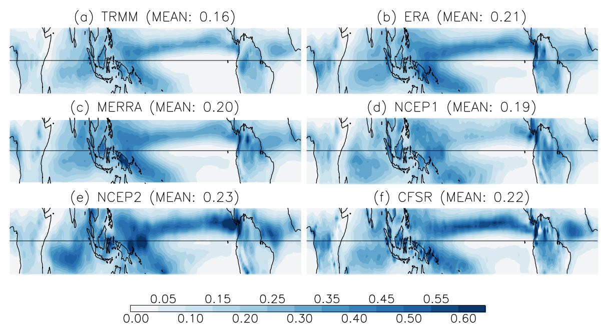

FIG. 1. Tropical mean precipitation (mm/hr) in 2005-2007 for (a) TRMM, (b) ERA, (c) MERRA, (d) NCEP1, (e) NCEP2, and (f) CFSR.

3. RESULTS

3.1 Mean precipitation

Fig. 1 shows that all reanalyses have positive biases in tropical precipitation. If the mean bias is subtracted, ERA and MERRA share similar characteristics with TRMM. NCEP1 shows a more spatially uniform distribution with less precipitation in the ITCZ compared to other datasets. In contrast, NCEP2 has a significant high bias in the ITCZ. CFSR also has strong precipitation along the ITCZ, but intensified precipitation distributions in the ITCZ are very different between NCEP2 and CFSR. While the positive bias of NCEP2 is significant in the western Pacific, precipitation along the ITCZ in CFSR is exaggerated mainly in the central and eastern Pacific.

3.2 Longitude-Time section

Fig. 2 shows zonal propagation of precipitation at 5N between June-September 2006. Observed TRMM precipitation in Fig. 2 (a) identifies the diurnal cycle and ubiquitous eastward and westward propagating features with different speeds. The large-scale eastward moving envelope is the Madden-Julian Oscillation (MJO). The active phase of the MJO is initiated in the Indian Ocean and progresses through the Maritime Continents and the western Pacific at the speed of 5 m/s. There are also

* *Corresponding author address:* Ji-Eun Kim, Univ. of Colorado, Dept. of Atmospheric and Oceanic Sciences, Boulder, CO 80309-0311; e-mail: jieunk@colorado.edu

smaller-scale eastward and westward waves within the MJO envelope.

In Fig. 2 (a), relatively faster eastward moving signals with the phase speed of about 10 m/s are Kelvin waves. Westward signals are composed of westward inertio-gravity (IG) waves and tropical depression (TD)-type waves, also known as “easterly waves”. Western African rainfall is dominated by small-scale westward propagation during northern summer, suggesting that the African Easterly Waves (AEWs), which are the TD-type waves in Africa, are strongly coupled to convection. The diurnal cycle is clearly seen over the land regions.

Fig. of 2 (b-f) show the same longitude-time cross sections for reanalyses. Precipitation patterns in ERA, MERRA, and NCEP1 are broadened in space and time. NCEP2, however, shows more intense and less broadened precipitation patterns. Westward propagations in NCEP2 are very significant compared to TRMM, especially in the eastern Pacific. CFSR in Fig.2 (f) has the most realistic variability and wave propagation characteristics.

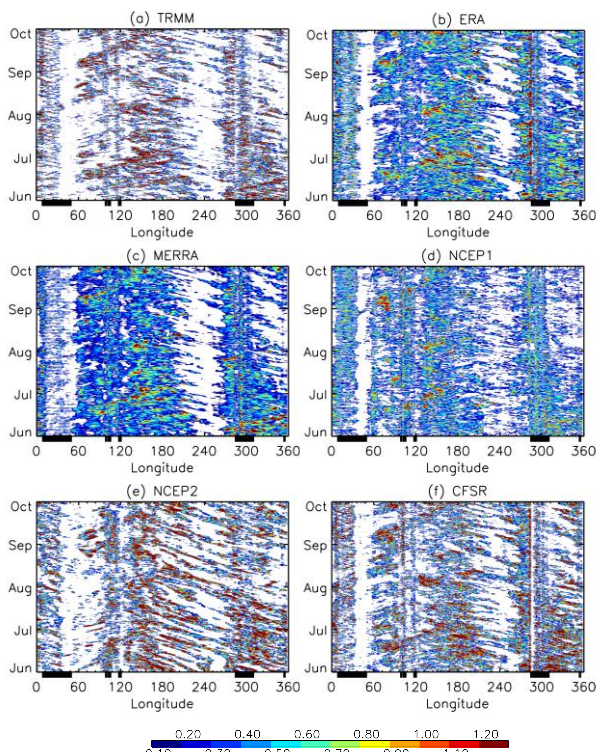

FIG. 2. Longitude-time section of precipitation (mm/hr) at the latitude of 5N between June-September 2006. Land regions are denoted by black bars in the longitude axis.

3.3 Spectrum

The raw spectra in Fig. 3 are very “red”, which means spectral density gets higher with lower wavenumber and lower frequency. The dotted lines correspond to the wave phase speeds. There is a prominent lobe in the eastward direction with the phase speed of about 15 m/s in the TRMM spectrum in Fig. 3 (a). This is mostly contributed by the Kelvin waves and the eastward IG waves. In the westward low-frequency range with periods longer than 7 days, the preferred westward phase speed is slowest and corresponds to the equatorial Rossby wave dispersion curve. As the frequency becomes higher in the westward direction, the preferred phase speed increases. At the higher-frequencies with periods shorter than 3 days, the prominent lobe follows along the phase speed of -18 m/s. Variability in this frequency range is contributed by the westward IG waves and the TD-type waves. Due to the Doppler shift by the westward zonal wind in the tropical troposphere, the phase speed of the westward IG wave mode is slightly faster than the value of the eastward IG wave. The intensified spectrum at the frequency of 1 CPD is due to the diurnal cycle.

The spectrum of each reanalysis in Fig. 3 (b-f) reveals its own characteristics and drawbacks. Generally, reanalyses have more “red” spectra than TRMM observations. At the frequencies lower than 1/3 CPD in ERA and MERRA, their preferred phase speeds are the same as TRMM. This suggests that the low-frequency planetary-scale CCEWs are well resolved in ERA and MERRA. However, they are lacking in wave signals at the frequencies higher than 1/3 CPD. Moreover, while the TRMM spectrum in the westward propagation direction is enhanced relative to the eastward direction at the frequencies, ERA and MERRA show only moderate enhancement of the westward part of the spectrum. This is a common problem in NCEP1, NCEP2, and CFSR. This weak enhancement in the westward disturbances suggests that all models used in reanalyses do not properly simulate the transient waves at the scales of IG waves and the TD-type waves.

NCEP1 and NCEP2 have spectra only up to 2 CPD due to the limitation of the time resolution. The striking feature of NCEP1 is the very strong diurnal cycle. The variance from the harmonics of the diurnal cycle in NCEP1 is 14 %, which is much higher than 3 % in TRMM. NCEP1 has the lowest spectral density and the highest diurnal cycle among all datasets. The spectral shape in the low frequencies shows weak CCEW signals compared to all other datasets. The spectrum of NCEP2 in Fig. 3 (e) has strong westward signals, but it is ambiguous to differentiate the Rossby and IG wave modes since the preferred phase speeds in Fig. 3 (e) look the same for these wave modes. In the positive wavenumber space in Fig. 3 (e), the Kelvin and eastward IG waves are found with the slower phase speeds than in TRMM.

The spectrum of CFSR in Fig. 3 (f) reveals that CFSR has improved skill in producing tropical precipitation in terms of the large-scale waves, high-frequency variability, and diurnal variations. Although CFSR is still lacking in wave signals at frequencies, the unrealistic strong westward signal in the planetary wave modes seen in NCEP2 has in CFSR become closer to the TRMM spectrum. The spectral power value of CFSR at higher frequencies is the most realistic compared to other reanalyses. The weak diurnal peaks in NCEP2 are also enhanced in CFSR to very reasonable values.

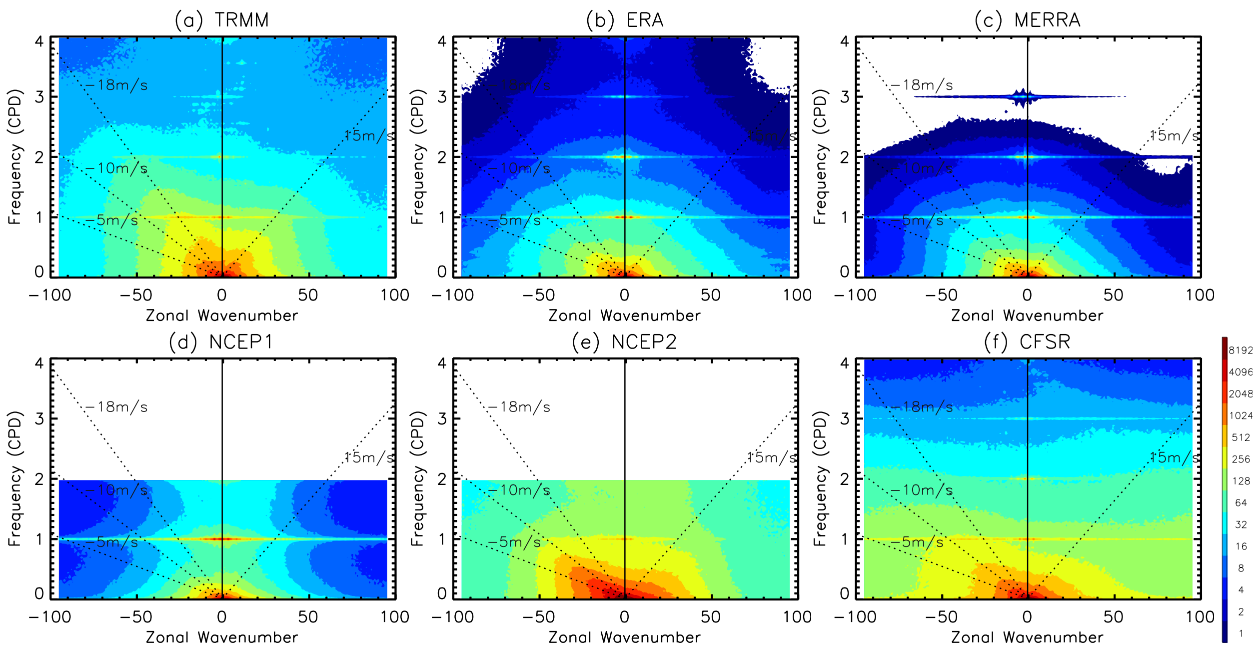

FIG. 3. Averaged wavenumber-frequency power spectrum of precipitation between 15S-15N over 2005-2007. Phase speed lines of -5, -10, -18, and 15 m/s are plotted with dotted lines.

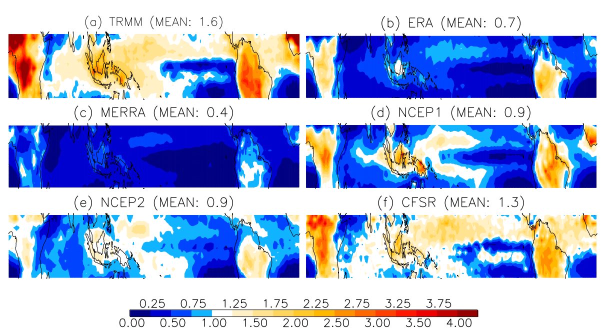

FIG. 4. Ratio of the high-frequency (periods < 3 days) variance to the low-frequency (periods > 3 days) variance.

3.4 Regional and Seasonal Variance

The ratio of the high-frequency variance (> 1/3 CPD) to the low-frequency variance (< 1/3 CPD) illustrates regional differences in the frequency characteristics in Fig. 4. Generally, over land, the impact of high-frequency precipitation variability is important. The ratios over land in all reanalyses, except in CFSR, are significantly lower than the ratio in TRMM. It appears that NCEP1 shows a good regional correlation of the variance ratio with TRMM, but this is because of the strong diurnal cycle in NCEP1. The lowest value of the mean ratio (See numbers in Fig. 4) in MERRA indicates that MERRA has the most persistent tropical precipitation. Although MERRA's representation of precipitation climatology has been improved compared to ERA and CFSR (Rienecker et al. 2011), the use of the relaxed Arakawa-Schubert scheme in the GEOS v.5.2.0 model for MERRA seems to result in significant lack of higher-frequency variability.

Fig. 5 shows seasonality of CCEW activity in different wave modes in seven regions. We divided the wavenumber-frequency spectrum into five categories:

- Q.-stat. (green): east- and westward >30days,
- WW_high (dark blue): westward < 3 days,
- WW_low (light blue) : westward > 3 days,
- EW_high (red) : eastward < 3 days, and
- EW_low (orange) : eastward > 3 days.

The MJO and the slowly moving Rossby wave signals with the period longer than 30 days are in the Q.-stat. category. We distinguished the high frequency from the low frequency with respect to 1/3 CPD (period of 3 days) so that the Kelvin, Rossby, and MRG waves are included in the low-frequency categories (Kiladis 2009). The contribution of the diurnal cycle is included in the high-frequency categories.

In TRMM observations, some regions such as Africa, the western and eastern Pacific, and America have obvious seasonal variations. While the WW_high variance largely varies with season, the lower frequency modes and the eastward IG wave modes do not have strong seasonal cycles.

Since the WW_high variance dominates the seasonal variation, we further investigate representation of WW_high variability in reanalyses in Fig. 6. The WW_high seasonal change in Africa in reanlyses generally matches the TRMM results, although the relative importance of the WW_high variance is different among datasets (See Fig. 6 (a)). The dominance of the WW_high variance in the western Pacific in Fig. 5 (d) implies that convection in northern summer is largely influenced by the IG and TD-type waves. Reanalyses generally do not capture well the seasonal enhancement of westward propagating convection in the western Pacific, shown in Fig. 6 (b).

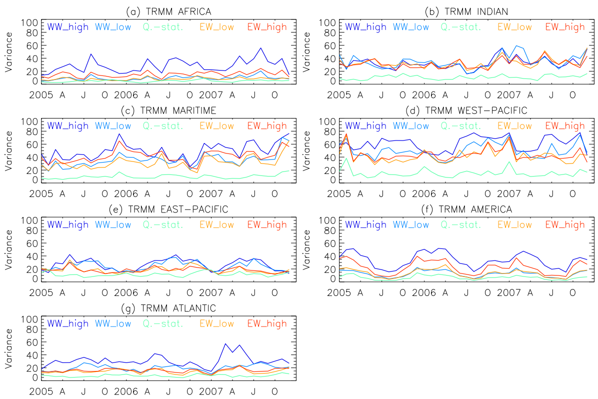

FIG. 5. Time series of TRMM regional precipitation variance (mm^2/hr^2) categorized according to propagation directions and frequency (westward_high: dark blue, westward_low: light blue, quasi-stationary: green, eastward_low: orange, and eastward_high: red).

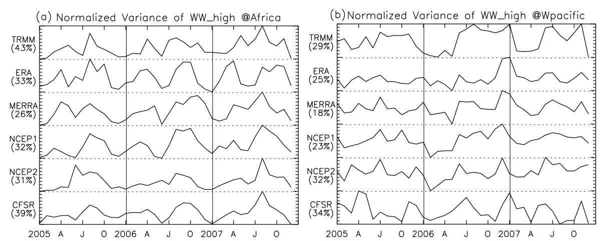

FIG. 6. Time series of normalized westward high-frequency variance in (a) Africa and (b) the western Pacific. The number in the parenthesis corresponds to the percentage of the westward high-frequency variance with respect to the total variance in a given region within a given dataset.

4. SUMMARY AND CONCLUSTIONS

Besides the common positive bias among reanalyses, the spectral analysis reveals deficiencies in resolving CCEWs and high-frequency variability. The low-frequency CCEWs are well represented in ERA, MERRA, and CFSR. At higher frequencies, however, all the reanalyses have no clear prominent lobes in the spectra, inferring no wave signals. The high-frequency variability in the reanalyses except in CFSR is weaker than in TRMM. Although there is no apparent signal of the convectively coupled IG or TD-type waves in CFSR, the high-frequency variance is comparable to TRMM.

The improvements in precipitation variability in CFSR are likely related to the use of the coupled model with fine resolutions. In addition, improvements of the high-frequency variability and diurnal cycle especially over land suggest that the direct assimilation of observed precipitation in the land surface model contributed to the better performance of CFSR.

It seems that ERA, MERRA, and CFSR can reproduce a realistic CCEW signal in low-frequency precipitation with the help of data assimilation of the observed state variables. At the higher frequencies, precipitation would depend more on the model than on observations due to lack of observations. Hence, the deficiency of high-frequency variability and wave signals in reanalyses may be improved by finer-scale observations and the improvement of the model physics.

It is worth of noting that NCEP2 uses the slightly modified version of the simplified Arakawa-Schubert convective parameterization scheme used in NCEP1, but their precipitation differs in many aspects. Our findings suggest that, along with the convective parameterization scheme, the choice for other model physics such as cloud processes, moist processes in the boundary layer, and the radiation scheme may also play important roles in CCEW activity.

This study confirms that the latest reanalyses such as ERA-interim, MERRA, and CFSR have much improved performance in resolving low-frequency CCEWs and precipitation variability over NCEP1 or NCEP2. However, the new reanalyses are still very different from observations with respect to variability and CCEW characteristics at high frequencies, meaning deficiencies in short-range forecasts.

Acknowledgments. This research is supported by NASA Ames Research Center contract #NNA10DF70C.

REFERENCES

Cho, H., K. Bowman, and G. North, 2004: Equatorial waves including the Madden-Julian oscillation in TRMM rainfall and OLR data. *J. of Climate*, **17,** 4387-4406.

Dee, D., and Coauthors, 2011: The ERA-Interim reanalysis: configuration and performance of the data assimilation system. *Quart. J. Roy. Meteor. Soc.*, **137,** 553-597.

Huffman, G., and Coauthors, 2007: The TRMM multisatellite precipitation analysis (TMPA): Quasi-global, multiyear, combined-sensor precipitation estimates at fine scales. *J. Hydrometeor.*, **8,** 38-55.

Kalnay, E., and Coauthors, 1996: The NCEP/NCAR 40-year reanalysis project. *Bull. Amer. Meteor. Soc.*, **77,** 437-471.

Kanamitsu, M., W. Ebisuzaki, J. Woollen, S. Yang, J. Hnilo, M. Fiorino, and G. Potter, 2002: NCEP-DOE AMIP-II reanalysis (R-2). *Bull. Amer. Meteor. Soc.*, **83,** 1631-1643.

Kiladis, G., M. Wheeler, P. Haertel, K. Straub, and P. Roundy, 2009: Convectively coupled equatorial waves. *Rev. Geophys.*, **47**, RG2003, doi:10.1029/2008RG000266.

Lin, J. L., and Coauthors, 2006: Tropical intraseasonal variability in 14 IPCC AR4 climate models. Part I: Convective signals. *J. Climate*, **19,** 2665-2690.

Rienecker, M., and Coauthors, 2011: MERRA: NASA's Modern-Era Retrospective Analysis for Research and Applications. *J. Climate*, **24,** 3624-3648.

Saha, S., and Coauthors, 2010: The NCEP climate forecast system reanalysis. *Bull. Amer. Meteor. Soc.*, **91,** 1015-1057.

Straub, K., P. Haertel, and G. Kiladis, 2010: An analysis of convectively coupled Kelvin waves in 20 WCRP CMIP3 global coupled climate models. *J. Climate*, **23,** 3031-3056.